# THE INTEGRATED DESIGN OF THE ITER MAGNETS AND THEIR AUXILIARY SYSTEMS*

M. HUGUET and the ITER Joint Central Team and the Home Teams
ITER Naka Joint Work Site, Naka-machi, Naka-gun, Ibaraki-ken, Japan

**Abstract**

The magnet system design for the International Thermonuclear Experimental Reactor (ITER) [1] has reached a high degree of integration to meet performance and operation requirements, including reliability and maintainability, in a cost effective manner. This paper identifies the requirements of long inductive burn time, large number of tokamak pulses, operational flexibility for the poloidal field (PF) system, magnet reliability and the cost constraints as the main design drivers. Key features of the magnet system which stem from these design drivers are described, together with interfaces and integration aspects of certain auxiliary systems.

## 1. INTRODUCTION

The International Thermonuclear Experimental Reactor (ITER) is described in the Final Design Report (July 1998) as a tokamak with a nominal plasma major radius of 8.1 m, plasma minor radius of 2.8 m, elongation of about 1.6 and plasma current of 21 MA. The toroidal magnetic field at the major radius is 5.7 T. The project goals include the demonstration of controlled ignition and extended DT burn in inductive pulses with a flat top duration of 1000 s. The expected average neutron loading at the first wall is 1 $MW/m^2$ and a total fluence of at least 1 $MW{\cdot}a/m^2$ is to be achieved for blanket and material tests [1-2].

The programme objectives establish a dual role for ITER. First, it must serve as a full scale test bed for the technologies of a fusion reactor and, therefore, provide the environment of a reactor core in terms of plasma performance, pulse duration, neutron flux and fluence, and expected activation. As a reactor test bed it must also have available a remote maintenance capability and it must offer attractive overall safety characteristics. Second, it must serve as an experimental facility with the flexibility to address and resolve open physics issues and to explore new operation domains with a view to optimizing the design of a demonstration fusion power reactor. This dual role is reflected in the operation plan which includes a Basic Performance Phase (BPP), essentially for experimental developments, and an Enhanced Performance Phase (EPP), with emphasis on nuclear operation. This dual role, however, results in conflicting requirements for the magnets, the design of which is a compromise between experimental flexibility and the simplicity and reliability expected for a reactor type of operation. It also makes it more difficult to observe cost constraints.

Detailed descriptions of the magnet design and R&D programme have already been given [3, 4] and are not repeated here. The paper identifies key design drivers in section 2. Sections 3 to 6 describe the impact of these design drivers on the magnet conceptual and detailed design. In sections 7 and 8, interfaces and integration issues in relation to the thermal shields, the cryostat and the cryoplant are reported. Cost considerations are addressed in section 9.

## 2. KEY FEATURES AND DESIGN DRIVERS OF THE MAGNET DESIGN

The magnet system is comprised of 20 Toroidal Field (TF) coils operating at a maximum field of about 12.8 T, a Central Solenoid (CS) which operates at a maximum field of 13 T, and 9 Poloidal Field (PF) coils operating at fields of typically 5 T. In addition, PF correction coils provide small components (about $10^{-4}$ of the toroidal field) of magnetic field to correct non-axisymmetric field errors. A mechanical structure provides support against gravity, electro-magnetic and seismic loads [2]. The magnet assembly is shown on figure 1. The magnet system is designed for up to 50,000 full power tokamak pulses. The magnets and structures are surrounded by thermal shields, which intercept radiation from surfaces at temperatures well above cryogenic temperatures, and are contained inside a cryostat which provides the vacuum for thermal insulation (Fig. 2).

---

* This report is an account of work undertaken within the framework of the ITER EDA Agreement. The views and opinions expressed herein do not necessarily reflect those of the Parties to the ITER EDA Agreement, the IAEA or any agency thereof. Dissemination of the information in these papers is governed by the applicable terms of the ITER EDA Agreement.

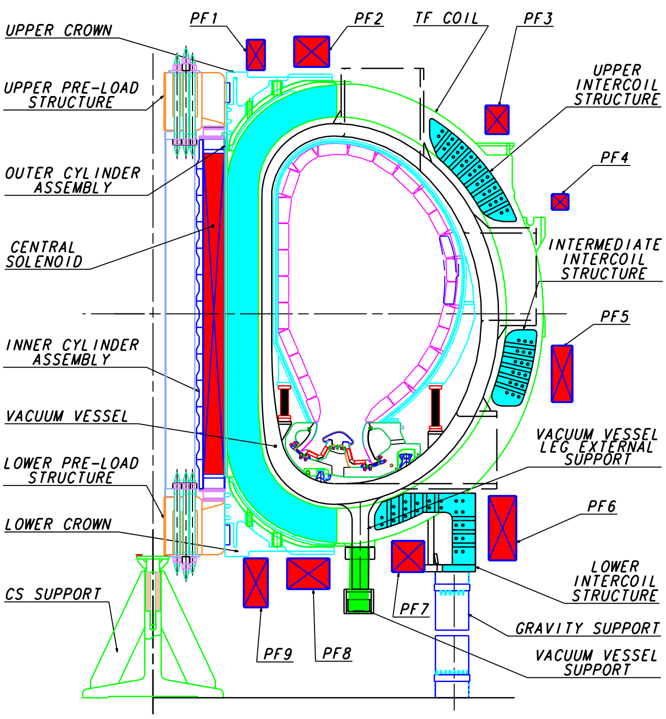


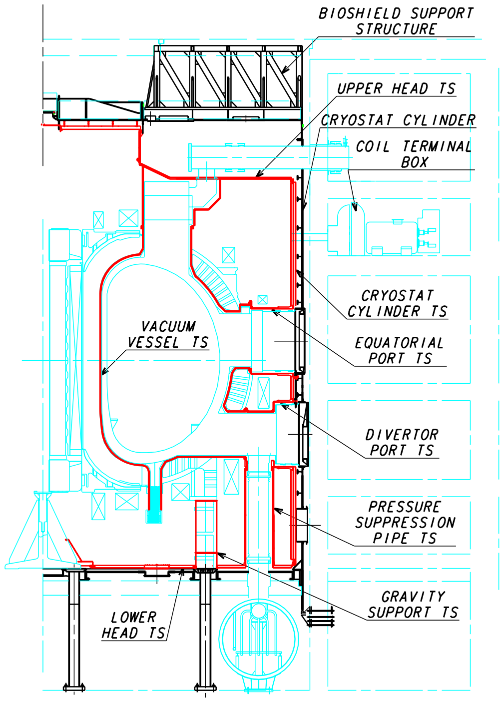


*FIG. 1. Elevation of magnet system showing coils and structures*

*FIG. 2. Elevation of machine showing Thermal Shields (TSs) and Cryostat*

All ITER coils are superconducting. In view of the high field requirement for the TF coils and CS, there was an early decision to use $Nb_3Sn$ superconducting material. This decision implied the need for a strong R&D programme to promote industrial development of this material and demonstrate coil manufacturing technology. This programme is well advanced and has been very successful in the industrial production of $Nb_3Sn$ superconductors and demonstrating the wind, react, insulate and transfer process. Model coils of the TF and CS types are nearly completed and testing is scheduled to start in 1999 [4]. For the PF coils, the use of NbTi at 4.5 K is technically possible except for one coil, PF9, which operates at a somewhat higher field and requires subcooling to 3.3 K. All coils use a cable-in-conduit type of conductor with supercritical He, forced-flow cooling. The conductor design and optimization is described elsewhere [5]. The conductor is the main cost driver for ITER magnets, and cost reduction measures are addressed in section 9.

Among the many requirements which have had a bearing on the magnet design, the key design drivers can be identified as the;

(1) requirement for an inductive pulse duration of 1000 s,
(2) requirement for a long lifetime of 50,000 full-power tokamak pulses,
(3) requirement for flexible operation of the PF system to allow a range of plasma profiles and scenarios,
(4) need for high operational reliability of the magnets, and
(5) cost constraints imposed to meet the overall Project cost limits.

As a result of the first requirement, the CS has to provide a large flux swing to produce a 21 MA plasma and sustain a 1000 s burn. For this reason, structures that take space and do not produce flux have been kept to a minimum in the centre of the machine. This has been achieved by bucking the TF coils onto the CS with the result that the CS is a monolothic, layer-wound coil since only this type of coil is able to provide a good bearing support for the TF coils. Another direct, and inevitable, consequence of this optimization philosophy is that structural limits are met in all components in the centre of the machine (section 4).

The second requirement confirms the choice of a bucked TF coil design which allows CS operation under mostly compressive hoop stress and hence the elimination of the fatigue issue for the CS. The TF coil cases, however, operate close to their fatigue limit (section 4).

The third requirement has been achieved with a PF coil system with a total of 9 coils. The ampere-turn capability of each PF coil has been determined to meet the demand of a wide range of plasma parameters and also a range of plasma scenarios. Details are given in section 3.

The fourth requirement stems from the fact that repair or replacement of magnets would require extensive machine down-time and ITER magnets must, therefore, achieve reliable, long term operation. Since the most common causes of magnet faults are insulation failures, specific, and sometimes unconventional, insulation design philosophies have been developed for the ITER magnets. Maintenance schemes have also been developed. Details are given in sections 5 and 6.

Cost drivers and design choices with a strong impact on cost are discussed in section 9.

## 3. A FLEXIBLE POLOIDAL FIELD COIL SYSTEM

The main development since the IAEA Conference in 1996 is the increase in the number of PF coils from 7 to 9 [6]. This has been achieved essentially by splitting the two small diameter PF coils, which were previously made with $Nb_3Sn$ superconductor. The result is a configuration with plasma shape and position control somewhat improved over the previous design. The main advantage, however, is a significant cost reduction because all PF coils now use NbTi superconductor (section 9).

As indicated in section 2, the CS is a monolithic, layer-wound coil with a fixed current distribution over its height. Alternative CS designs which allow changing this current distribution have been evaluated. The main option considered was a CS segmented into three, independently powered modules along the vertical axis. This option offered plasma shaping advantages and, in particular, the possibility to increase the plasma triangularity above the reference value of 0.24 to about 0.29. Steady-state operation was also improved in terms of plasma shaping capability (range of achievable $l_i$ values). However, the segmented CS design could not be selected because of higher than allowable stress in three critical areas in the center of the machine (section 4). The monolithic, layer-wound solenoid design has therefore been retained because it fulfills the ITER mission.

The location and size of the PF coils have been optimized for the nominal 21 MA plasma current scenario taking into account a wide range of plasma pressure and current profiles ($0 \leq \beta_p \leq 1.2$ and $0.7 \leq l_i \leq 1.1$). This optimization included the requirements to control the plasma in the event of large plasma disturbances at different phases of the scenario. The control system is designed to recover the plasma shape and position after plasma disturbances characterized by $|\Delta\beta_p| \leq 0.2$ and/or $|\Delta l_i| \leq 0.1$. Plasma disturbances with larger magnitudes ("giant" sawteeth, "giant" ELMs, H-to-L mode transitions during the burn, major disruptions) are also expected, but the strict maintenance of shape following such events is not considered mandatory.

In addition to the nominal scenario, the PF system can support other scenarios including:

- heating during plasma current ramp-up in the 21 MA scenario;
- different ramp-up rates in the 21 MA scenario;
- accelerated plasma termination (150 s) in the 21 MA scenario;
- high current (24 MA) scenario with a shorter inductive flat top of 560 s;
- long inductive burn (4500 s) scenario at a current of 17 MA;
- 12 MA steady-state scenario with reversed shear.

## 4. A COMPACT STRUCTURAL DESIGN

The design has been optimized to achieve a 1000 s long inductively-driven burn time. As a result, the TF coils are bucked on the CS and there is only a very thin structure, the Outer Cylinder (OC), at the interface between the external surface of the CS and the noses of the TF coil cases. The "bucked" design, as opposed to a "wedged" design where the TF coils form a self-supporting vault, saves space in several ways: the structural steel in the CS can be reduced since the CS operates under mostly compressive hoop stress, and fatigue (in relation to the 50,000 full-power tokamak cycles which correspond to 100,000 CS full field energizations), is not an issue; there is no need for a thick steel structure at the nose of the TF coils to react the radial centripetal load. For ITER, it was estimated that a bucked design results in a major radius about 0.5 m smaller than a wedged design. As already indicated in section 2, the bucked TF coil design requires a layer-wound CS which provides a structurally axisymmetric and vertically uniform bucking support with a smooth outer surface free from geometrical discontinuities due to electrical terminals, joints and coolant supply lines.

The 20 TF coil cases form the main structural component of the ITER tokamak and integrate all coils and the Vacuum Vessel (VV) into a single mechanical system (Fig. 1). The PF coils and the VV are directly supported in the vertical and horizontal directions by the TF coil cases. This is important for seismic and electromagnetic loads and, in particular, for Vertical

Displacement Events (VDEs) which generate large vertical and horizontal loads on the VV. These loads are equilibrated within the magnet structure and are not transferred to external structures. This concept of a compact load containment, where load paths are kept as short as possible, allows the minimization of stress, of displacements under load, and of volumes of supporting structures.

The forces on the TF coils arising from the interaction with the poloidal field (out-of-plane forces) are supported by the TF coil cases and the three outer intercoil structures which are integral parts of the TF coil cases. These structures are located on the outboard legs of the coils and are very rigid against torsional deformations. Additional out-of-plane support is provided by two crowns at the upper and lower inboard curved regions of the TF coils. Along the straight inboard legs of the TF coils, the out-of-plane deflection is transferred to the CS by friction. The torsional stiffness of the CS, however, contributes only marginally to the out-of-plane support for the TF coil inboard legs.

Structural analyses cover a wide range of operating conditions, including seismic and off-normal events. The results show that the magnet system fulfills the requirements with safety margins on maximum stress and fatigue life according to design criteria, but that there are three areas where stresses are close to the allowed limits:

(1) the lower inboard curved regions of the TF coil case where there is a combination of hoop tension, in-plane and out-of-plane bending. In this region, the maximum principal stress for fatigue assessment reaches 435 MPa and the cyclic component of stress generated by out-of-plane bending is 245 MPa. Such stress levels are acceptable for a high strength austenitic stainless steel with minimum 4K properties of 1000 MPa for the 0.2% offset yield strength and 200 Mpa·m for the fracture toughness.

(2) the lower crown and the TF coil cases have high local stresses at their inner radius interfaces. This is due to the relative lack of out-of-plane support along the TF coil inboard legs which results in a concentration of reaction forces at the inner radius of the crown.

(3) the CS experiences shear due to the combined effect of torsion from the TF coils and bending over the height due to the non-uniform TF centering force. The most critical load is the torsional shear which is driven by the out-of-plane deflection of the TF coil inboard legs and transferred to the CS by friction. Torsional shear reaches 31 MPa in the equatorial plane region, and is just within the allowable limit for the chosen insulation system which uses epoxy, glass and polyimide tape.

All the high stresses are a direct consequence of the design optimization philosophy to maximize the flux swing generated by the CS and therefore minimize structures in the centre of the machine. The high stresses are generated by the out-of-plane loads acting along the TF coil inboard regions and, in particular, in the divertor region where the poloidal flux transverse to the TF coils is relatively large. These stresses are very sensitive to the load distribution. For example, attempts to increase the plasma triangularity by means of a non-uniform current density in a segmented CS have been unsuccessful as the out-of-plane load distribution becomes more severe and stresses in all three critical regions substantially exceed allowed limits. Studies related to a reduced cost version of ITER have confirmed that an increase of the plasma elongation and triangularity above the reference values can be achieved but requires a more rigid support of the TF coil inboard legs. Such higher rigidity is achievable with a much thicker Outer Cylinder and stiff torsional links between the Outer Cylinder and the crowns but is not compatible with the CS flux swing requirements unless the radial built, and therefore the cost, of the machine is increased.

## 5. MAGNET ELECTRICAL INSULATION : A KEY FACTOR FOR RELIABILITY

Magnets are permanent components of the ITER machine and must be designed to achieve maximum reliability and a fatigue life compatible with at least 50,000 full-power tokamak pulses. Many design and manufacturing quality aspects have a bearing on magnet reliability, but experience with magnet operation indicates that the most common causes of magnet faults are insulation failures. In this section, the discussion is restricted to the specific insulation design philosophies which have been developed for ITER magnets.

The magnet reliability relies on three lines of defense:

(1) design and strict manufacturing QA to make a fault very unlikely.

(2) damage induced by a fault, should it occur, is mitigated by design. This implies that the detection of insulation faults must be possible before significant consequential damage occurs.

(3) in the event that a) and b) above have not been effective, recovery options are available allowing (depending on the type of coil) the by-pass of the faulty section of a magnet

(possible for the PF coils) and/or local repair. In the worst case, replacement of any coil is possible.

In accordance with point (1) above, the ITER magnet insulation reliability is greatly improved though the use of a material with intrinsically good dielectric properties, i.e., a polyimide film, which provides a full electrical barrier without the need to rely on the quality of the vacuum impregnation with epoxy resin.

**The TF coil insulation system :** The TF coils use a thin-jacketed circular conductor embedded in grooves machined into "radial plates" (Fig. 3). This arrangement offers the following advantages as compared to a conventional thick-walled square conductor winding pack:

(1) the Lorentz forces acting on each conductor are directly transferred to the radial plate and there is no accumulation of these loads on the conductor insulation.

(2) insulation on circular conductor is much more robust than on square conductors due to the absence of corners. Conductor corners and the gap where corners of adjacent conductors meet are critical regions with stress concentrations and poor control of the insulation quality.

The radial plate design results in a TF conductor insulation which is mechanically and dielectrically very robust and can easily stand the coil full ground voltage. Considering that the radial plates form a physical separation between the turn insulation and the coil ground insulation, the TF coils are provided with a redundant insulation system. In addition to redundancy, the radial plates ensure that a short between conductor and plate, should it occur, would be detected and would not produce any further damage. This is achieved by monitoring the insulation resistance between conductor and plate.

**The PF coil insulation system :** The design objective has been to eliminate the risk of internal shorts (between turns or pancakes). Internal shorts could produce extensive damage with local melting of the superconducting cable and its conduit and the only possible remedial action would require the faulty coil module to be cut up and physically removed. To eliminate the risk posed by shorts, all PF conductors are provided with a double insulation which (except for PF1 and PF9) is composed of an internal insulation layer, an intermediate steel foil wrap (0.2 mm) and an outer insulation layer. With this configuration, the failure of one of the two insulation layers can be detected by the foil wrap, the potential of which is accessible through a current limiting resistor. In this event, the affected coil module can be electrically by-passed thus allowing operation to continue without the need for a major intervention inside the cryostat. It is important to note that operation with a by-passed module can continue at full power because there is a built-in redundancy in the PF coil design, whereby each coil consists of 4 identical modules allowing full ampere-turn operation of the coil with 3 modules only, but at reduced operating temperature (3.8 K).

**The CS insulation system :** Due to space restrictions and the need to achieve a high current density in the winding pack, double insulation has not been used in the reference design for the CS conductor. The provision of a high quality conductor insulation relies on wrapping and curing this insulation prior to assembly of the conductor into the coil thus allowing full visual inspection and HV test of the conductor insulation. The use of double insulation remains, however, an option but would result in some cost increase and a small reduction of the flux capability.

The short circuit of an entire TF coil represents a serious risk for the tokamak in view of the potential damage due to stored energy deposition and electromagnetic forces. This risk must be eliminated not only to protect the tokamak but also for safety reasons to ensure that the confinement barriers, the VV and the cryostat, are not at risk from such an accident. For these reasons, the TF coil terminals and feeders have been provided with double insulation as described for the PF coil conductors. In addition, the terminals and feeders are separated by a steel plate thick enough to carry the current from a ground short.

## 6. MAGNET MAINTENANCE RELIES ON HANDS-ON INTERVENTIONS

Although ITER magnets and all magnet components inside the cryostat are designed to last the lifetime of ITER without requiring inspection or maintenance, plans are available for repair should it become necessary [7]. Interventions fall into 2 categories: 1) relatively brief access to the so-called “break boxes” for minor repair and 2) major interventions for an entire coil replacement. This paper considers only the minor interventions which are more likely, but it must be stressed that replacement schemes have been conceptually developed for all ITER magnets.

For minor interventions, the strategy is to use hands-on maintenance [8]. Remote maintenance is considered only as a back-up during the EPP if radiation levels preclude human access. To support this hands-on strategy, the radiation shielding has been optimized such that the expected dose on the external surfaces of the magnets is about 200 μSv/hour thus making time-limited, controlled personnel access inside the cryostat possible until the end of the BPP, and possibly later.

The coil break boxes are located close to the coil surfaces inside the cryostat and contain terminal joints, helium manifolds, insulating breaks in series with cooling pipes and instrumentation. A typical intervention would involve the replacement of the insulating break of a helium coolant pipe. The coil break box locations have been optimized to allow man access. Permanent access platforms, walkways, lifting points and other features to simplify and reduce the duration of in-cryostat maintenance operations have been integrated into the magnet and cryostat designs. Access into the cryostat is provided by a number of ports at the top, the cylindrical surface, and bottom of the cryostat, in locations which allow direct access to coil break boxes. The box internal design provides easy reach to components which may require maintenance and takes into account space requirements for automatic cutting and welding tools.

## 7. THERMAL INSULATION OF THE ITER MAGNETS

The magnet thermal insulation is provided by two thermal shields, the vacuum vessel thermal shield and the cryostat thermal shield, and a cryostat which contains the whole tokamak (Fig. 2).

The vacuum vessel thermal shield is located in the narrow gap between the TF coils and the VV. The key design issues for this thermal shield were :

(1) to minimize the thickness of the shield and the gap between the TF coils and the VV at the inboard region taking into account thermal and mechanical relative displacements;

(2) to ensure no line of sight between the VV and the coils and minimize radiation from the shield to the coils.

The design solution is a shield which is a thin, stainless-steel, self supporting, toroidal shell. The shield is no more than 53 mm thick and fits within a 120 mm gap, at assembly, between the TF coils and the VV at the inboard region. The shield is cooled by helium gas at 80 K and is silver-plated on both sides for low emissivity; the radiative heat load from the shield to the magnets is of the order of 1 kW. The shield includes 80 toroidal breaks of which 60 are electrically insulated to reduce eddy currents and associated magnetic forces. There are also 2 poloidal electrical breaks. The shield is hung from the TF coil cases and the design has been integrated such that one TF coil and a shield sector form a single unit for assembly. The cryostat thermal shield is supported from the cryostat walls and located close to these walls to ease in-cryostat access. This shield is composed of a steel frame which is cooled by helium gas at 80 K and panels which are welded or bolted to the frame. The panels are steel plates which are copper clad to achieve a uniform temperature distribution and silver plated for low emissivity. The vacuum vessel and cryostat thermal shields are connected by additional shields around the vessel ports, vessel supports and the machine gravity supports [2].

The tokamak is installed inside a large (32,700 $m^3$) vacuum vessel, the cryostat, which provides the vacuum for the thermal insulation of the magnets and structures and forms part of the tokamak second confinement barrier. It is designed to survive, without damage, the accidental loss of magnet helium coolant. The cryostat has a flat lower head and a flat upper head to reduce building height and cost. The upper head is integrated with the top biological shield supports which consist of steel truss structures. The gravity support ring pedestal provided at the cryostat lower head is connected to the tokamak gravity supports by bolts, and supports the entire tokamak machine loads. The cryostat provides ports and penetrations with bellows to access the vacuum vessel. There are many access ports to the cryostat interior in the upper head, on the lower half of the cylinder and on the lower head [2].

## 8. THE MAGNET PULSED HEAT LOADS : A CRITICAL ISSUE FOR THE CRYOPLANT

The magnets and structures are cooled in closed loops by forced flow of supercritical helium at about 4.5 K. The loops include heat exchangers immersed in LHe baths from which the evaporating helium is extracted by cold compressors and rejected into the process loop of the cryoplant. The heat load can be broken down into :

(1) a static refrigeration load as a result of conduction and radiation,

(2) a pulsed refrigeration load due to AC losses in conductors, eddy current losses in structures, nuclear heating and mechanical friction losses in structures. The circulation pumps and cold

compressors work is also a variable load which depends on the mode of operation of the machine.

(3) a liquefaction load for current leads cooling.

At nominal power and pulse repetition rate, the total time-averaged refrigeration load is 84 kW of which about 39 kW is pulsed. The liquefaction load is 0.19 kg/s. The key issue of the cryoplant design is to smooth the large pulsed heat load to make it compatible with the cryoplant which is essentially a steady-state device. This is achieved by a combination of measures as follows. The large inventory of helium in the coils (about 210 $m^3$) acts as a thermal buffer. The tokamak structural components, the crowns and to some extent the TF coil cases, are also used as thermal buffers. To this end, the helium flow is controlled to allow a temperature rise, within allowed limits, of these structural components during a plasma pulse. A major load buffering action is provided by controlling the cold compressors such that the power extracted from the LHe baths is kept constant or slowly varying. A 40 $m^3$ LHe buffer tank provides additional load smoothing by allowing the cryoplant to switch from a refrigeration to a liquefaction operation mode and vice versa. With these provisions, the process loop of the cryoplant is only required to respond to slowly-varying loads and this is achievable by warm compressor control and control of the process loop pressure.

The full cryoplant is expected to include 8 LHe plant modules each of 11.75 kW plus 0.034 kg/s, operated in parallel [2]. This module size is proposed in order to use the experience gained with the 18 kW refrigerators of CERN for the superconducting ring of the Large Hadron Collider. The initial investment can be reduced since 6 LHe plant modules are sufficient to satisfy the plasma operation requirements for several years until long burn D-T operation is established.

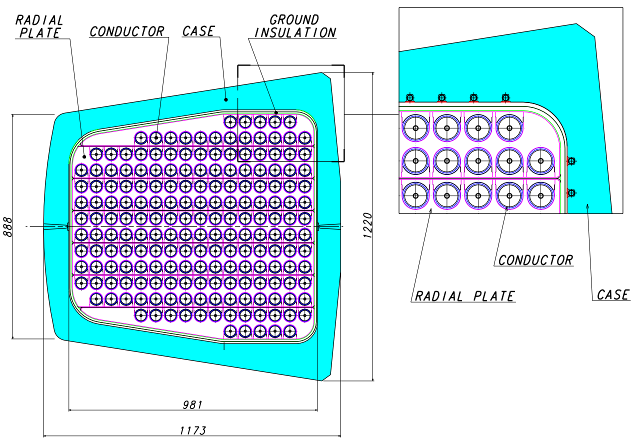


*FIG. 3. Cross section of TF coil and detail showing conductor in radial plate slots*

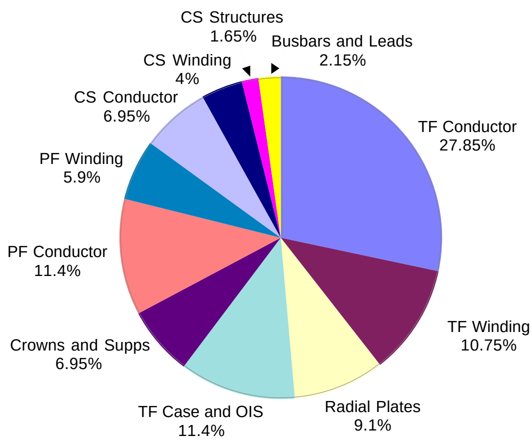


*FIG. 4. Magnet cost breakdown*

## 9. COST DRIVERS AND COST REDUCTION OPTIONS

The FDR Magnet Systems require about 1040 t of $Nb_3Sn$ strand, 865 t of NbTi strand, 657 t of copper wire, 2411 t of stainless steel conduit, 884 t of Incoloy 908 conduit, and about 19,000 t of stainless steel structures. The total magnet system cost of 1,800 kIUA (1 IUA=1 US k$ at 1989 value) is about 33 % of the total Project investment cost. The pie-chart in Fig. 4 shows the relative costs of the main components. Forty six percent of the total magnet system cost is in the conductor. The bulk of the finished conductor cost for any coil is in the strand and the cost of $Nb_3Sn$ strand is about 3.6 times the cost of NbTi strand on a weight basis. It is clear that the focal points of cost reduction efforts should be a) the conductor and particularly the TF conductor since this cost is about 28 % of the total magnet system cost; b) the TF coils including the winding, radial plates, cases and outer intercoil structures.

Cost minimization has driven the change from a PF coil configuration with 7 coils to a configuration with 9 coils. A PF coils total cost reduction of about 13 % resulted from the ability to use NbTi superconducting material for all nine PF coils, whereas, the previous configuration required the use of $Nb_3Sn$ in 2 coils. The increase in the quantity and cost of NbTi is small compared to the cost decrease resulting from the elimination of $Nb_3Sn$ conductor and of the more complex manufacturing requirements for two $Nb_3Sn$ PF coils. The main effort to minimize cost has been focused on the TF coil conductor. The use of an Incoloy 908 jacket, rather than a steel jacket, for this conductor results in improved strand performance and reduces the required strand quantity by 15 to 20%. This is because the thermal expansion of Incoloy 908 matches that of $Nb_3Sn$ and there is no reduction of critical current and field due to thermally applied strain. Incoloy 908 has also been used for the CS not only for cost reasons but also to achieve the required flux swing. Further significant reductions in $Nb_3Sn$ strand quantities can be achieved. A reduction of design margins is deemed possible in view of the experience gained during the strand production and R&D development for the ITER Model Coils. Measures include a reduction of the temperature margin from 2 to 1 K and the use of a higher heat exchange coefficient between copper and helium. This should result in an overall ITER conductor cost reduction of about 16% [9]. This has been evaluated after the issue of the ITER Final Design Report.

The TF coil winding pack includes radial plates which are expensive components to manufacture because of the requirements for extensive machining and tight dimensional tolerances. Figure 4 shows that the cost of radial plates is about 9 % of the total magnet cost. A choice could, therefore, be made between 3 basic options: a) a winding pack with radial plates and a conductor with a thin incoloy 908 jacket; b) a winding pack without radial plates and a conductor with a thick-walled, square Incoloy 908 jacket; c) same as b) but with a stainless steel jacket. The costs of options a) and b) have been found to be similar because the manufacturing cost of radial plates is about the same as the cost of the thick-walled incoloy jacket. Option b) is, however, problematic since it implies, for the TF coil cases, the use of a material with a low contraction coefficient to match the Incoloy properties. The cost of option c) is close to that of both options a) and b) because the low cost of the stainless steel jacket is offset by the larger quantity of strand required. Option a) was, therefore, selected on the basis of the reliability advantages described in section 5.

Cost constraints can be in conflict with reliability and flexibility requirements. Section 3 has shown that the PF coil ampere-turn capability has been determined to meet the demand of a wide range of plasma parameters and scenarios. As a result, the PF coils are oversized for any specific plasma scenario. Moreover, the PF coils include a 25% redundant ampere-turn capability to allow operation at full performance after the occurrence of a fault necessitating the by-pass of one of the four modules constituting a coil. In this case, the flexibility and reliability requirements have taken priority over cost considerations.

## 10. CONCLUSIONS

The ITER magnet system has been able to meet the challenging set of performance and operation requirements imposed by the Project objectives. Reliability and maintenance requirements have also been given a high priority. In order to fulfill all these, often conflicting, requirements within strict cost constraints, a rigorous design optimization philosophy has been followed. For example, the 1000 s long inductive burn time and the 50,000 pulses requirements are met, but as a consequence, structural limits are reached in several components in the centre of the machine. Auxiliary systems and their interfaces with the magnets have been highly integrated, resulting in space savings, cost reductions and reliability improvements. The magnet system in the ITER Final Design Report represents an optimum design for the specific requirements of the ITER Engineering Design Activity.

## References


[1] SHIMOMURA, Y., ITER Overview, this conference.

[2] TECHNICAL BASIS FOR THE ITER FINAL DESIGN REPORT, COST REVIEW AND SAFETY ANALYSIS (FDR), IAEA/ITER EDA/documentation series (1998), to be published.

[3] HUGUET, M., The ITER Magnet System, Fusion Engineering and Design, Vol. 36 (1997) 23-32.

[4] THOME, R.J., BARABASCHI, P., Recent Progress on the ITER Magnet Systems, Proceedings of the 17th IEEE/NPSS SOFE, San Diego, California (1997) pp 427.

[5] MITCHELL, N., BESSETTE, D., Conductor Development for the ITER Magnets, 15th Magnet Conference, Beijing, China (1997).

[6] MONDINO, PL., ITER Plasma Shaping Capability: Comparison of Alternative Magnetic Configurations, Proceedings of the 17th IEEE/NPSS SOFE, San Diego, California (1997) pp 633 - 636.

[7] HAANGE, R., et al., Remote Handling Maintenance of ITER, this conference.

[8] TESINI, A., et al., Repair of Components Located Inside the ITER Cryostat: Engineering and Safety Aspects, Proceedings of the 20th Symposium on Fusion Technology, Marseille (1998), pp 1107 - 1110.

[9] BESSETTE, D., Towards Less Expensive Conductors for the ITER Magnets, Proceedings of the 20th Symposium on Fusion Technology, Marseille (1998), pp 799 - 802.